

Photothermal sensitisation as a novel therapeutic approach for tumours: Studies at the cellular and animal level

Monica Camerin ^a, Santiago Rello ^b, Angeles Villanueva ^b, Xinzhan Ping ^c,
Malcolm E. Kenney ^c, Michael A.J. Rodgers ^d, Giulio Jori ^{a,*}

^a *Department of Biology, University of Padova, Via Ugo Bassi 58 B, 35121 Padova, Italy*

^b *Department of Biology, University of Madrid, Spain*

^c *Department of Chemistry, Case Western Reserve University, Cleveland, OH, USA*

^d *Department of Chemistry, Bowling Green State University, Bowling Green, OH, USA*

Received 16 December 2004; received in revised form 27 January 2005; accepted 2 February 2005

Available online 18 April 2005

Abstract

Irradiation of B78H1 murine amelanotic melanoma cells with 850 nm light emitted from a Ti:sapphire laser, operated in a pulsed mode at high fluence rates and in the presence of Ni(II)-octabutoxy-naphthalocyanine (NiNc), promoted a photothermally sensitised process leading to fast and irreversible cell death. This resulted in the ejection of a consistent mass of cytoplasmic material from the irradiated cells that was detected by scanning electron microscopy. The extensive chemical and mechanical damage was probably caused by the photoinduced generation of an acoustic shock wave. The efficiency of the photoprocess was modulated by intracellular concentration of NiNc and maximally by the formation of aggregated naphthalocyanine clusters in specific subcellular areas. Very similar results were obtained upon irradiation of NiNc-loaded C32 human amelanotic melanoma cells and transformed murine HT-1080 and HaCaT fibroblasts. From these results, photothermal sensitisation appears to be a general phenomenon and preliminary studies with mice bearing subcutaneously transplanted amelanotic melanomas, irradiated with 850 nm light 24 h after intravenous injection of NiNc, suggest that this approach has potential for the therapy of some types of skin tumours.

© 2005 Elsevier Ltd. All rights reserved.

Keywords: Phototherapy; Photothermal; Photosensitisation; Pulsed irradiation; Lasers; Naphthalocyanines; Tumours; Amelanotic melanoma

1. Introduction

Photodynamic therapy (PDT) is becoming an established treatment for selected neoplastic lesions, especially after the recent approval by the Food and Drugs Administration USA, of Photofrin-based PDT [1] and the advent of 5-amino-levulinic acid (ALA). ALA is a prodrug that generates the photosensitising agent protoporphyrin IX in tumour cells through the stimulation of

endogenous metabolic processes [2]. So far, the majority of thousands of patients that have been treated with PDT have objectively benefited from the therapy [3]. At the same time, PDT is also being considered as a treatment tool for several cutaneous diseases [4], microbial infections [5], and the prevention of restenosis after balloon angioplasty [6]. The introduction of second-generation photosensitising agents, with superior photophysical and pharmacokinetic properties compared with porphyrins, is also increasing the potential of PDT as a treatment choice [7]. In spite of these positive features, some limitations appear to be associated with PDT [1,2], which can be partially overcome by

* Corresponding author. Tel.: +39 049 8276333; fax: +39 049 8276344.

E-mail address: jori@bio.unipd.it (G. Jori).

combining it with other therapeutics such as chemotherapy [8] or radiotherapy [9].

Recently, we proposed a variant of PDT, namely photothermal therapy (PTT), as a novel approach for the treatment of tumours [10]. The approach is based on the promotion of photothermally sensitised processes in tumour cells or tissues. In general, photothermal processes reflect the tendency of a light-absorbing species to dissipate electronic excitation energy via a rapid cascade through vibrational modes resulting in increased kinetic energy of the matrix species around the chromophore, i.e., to heat the local environment. The temperature rise can reach 130 °C above the basal value [11]. Under these conditions, water molecules tend to vaporize setting up an acoustic shock wave that propagates through the medium causing both mechanical and chemical alterations in the system. In some molecular absorbers, radiationless decay to the ground state and heat generation occur on a picosecond time scale [12]. Using laser pulses of high fluence rates (e.g., 1 J cm^{-2} in 10 ns) allows the possibility of absorption of other photons in the same volume before the first temperature spike has suffered much dissipation. This then creates the conditions for increased shock wave activity and subsequent damage to cell/tissue components. These effects could be further potentiated in biological systems when suitable chromophores are present at high local concentrations due to aggregation or compartmentalisation. Simultaneous photoexcitation events could lead to two or more thermal spikes in close proximity with concomitant generation of more vigorous shock waves and greater damage. A few endogenous constituents of cells and tissues, such as melanin and oxyhemoglobin, can act as starting points for the promotion of photothermal processes, and this property has been used in clinical practice for the fading of cutaneous lesions such as nevi or *café-au-lait* macules [13] or the removal of port-wine stains [14]. However, the scope of photothermal sensitisation is not necessarily limited to the treatment of diseased tissues containing natural chromophores. Dyes such as cyanines, azo-dyes, triphenylmethane derivatives and porphyrins coordinated with transition metal ions exhibit photophysical features that are suitable for photothermal sensitisation [15]. The introduction of exogenous photothermally acting chromophores that localise preferentially in diseased tissues could provide a novel therapeutic approach. Indeed, photothermal therapy of cancer lesions using a combination of *in situ* administered indocyanine green and a near-infrared laser has been previously described [16,17].

The available lines of evidence suggest that PTT [10,15] could have either specific applications or act synergistically with PDT. In PDT, where photogenerated hyper-reactive oxygen species are the main cytotoxic intermediates, cell death is less efficient in tumours that are poorly vascularised, owing to insufficient oxygen lev-

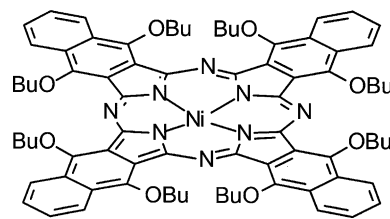


Fig. 1. Chemical structure of Ni(II)-5,9,14,18,23,27,32,36-octabutoxy-2,3-naphthalocyanine (NiNc).

els in the neoplastic tissue [18]. However, in PDT photothermal sensitizers appear to efficiently induce malignant cell death even in the absence of oxygen [19]. Furthermore, PTT can also be usefully applied [20] in cases of highly pigmented tumours, such as melanotic melanoma, where PDT yields unsatisfactory results due to light-filtration by melanin [1,3]. In view of the clinical potential for PTT, it is important to investigate the mechanisms by which photothermal sensitisation acts at the cellular and tissue level. In this paper, we present the first set of observations on the processes involved in the photothermal inactivation of tumour cells sensitised by Ni(II)-octabutoxy-naphthalocyanine (NiNc) *in vitro* and *in vivo*. This naphthalocyanine (Fig. 1) is endowed with favourable properties to act as a photothermal sensitizer [15], including a large molar extinction coefficient in the 800–850 nm spectral region where most human tissues exhibit a high relative transparency to light [21], a very short lifetime of the electronically excited states, an efficient conversion of electronic into thermal energy and a high affinity for tumour cells that is typical of several phthalocyanines [22].

2. Materials and methods

2.1. Photosensitizer and liposomal formulation

Ni(II)-5,9,14,18,23,27,32,36-octabutoxy-2,3-naphthalocyanine (NiNc) was prepared according to standard methods [23] and its purity was found to be greater than 98% by elemental analysis and NMR. The naphthalocyanine concentration was determined spectrophotometrically using an extinction coefficient of $280\,000 \text{ M}^{-1} \text{ cm}^{-1}$ at 848 nm in tetrahydrofuran [24]. NiNc was added to the cells or injected *in vivo* after incorporation into small unilamellar vesicles of DL- α -dipalmitoyl-phosphatidyl-choline (DPPC, Sigma, 99% pure), which were prepared according to a modified protocol of the ethanol injection procedure developed by Kremer and colleagues [25]. Typically, 0.75 ml of an ethanol–tetrahydrofuran binary mixture (1:1, v/v), which was 9.56 mM in DPPC and 0.27 mM in NiNc, was injected into 10 ml of a 0.9% (w/v) aqueous solution of NaCl regulated at 55 °C. The NiNc appeared to be in a purely monomeric state inside

the liposomes and the suspension thus obtained was stable for at least 24 h as judged by the lack of appreciable variations in the visible absorption spectrum.

2.2. Studies of cell accumulation and subcellular distribution

Four tumour cell lines, as shown in Table 1, were studied. B78H1, HT-1080 and HaCaT cells were grown in Dulbecco's modified minimal essential medium (D-MEM, Sigma) containing 10% heat-inactivated foetal calf serum (FCS, Boehringer, Mannheim, Germany) and supplemented with 100 units/ml penicillin, 100 µg/ml streptomycin and 0.25 µg/ml amphotericin. C32 cells were grown under identical conditions but using minimal essential medium containing non-essential amino acids (Gibco). The cell lines were routinely checked for the absence of mycoplasma contamination.

For photosensitizer accumulation studies, $2.5\text{--}5 \times 10^5$ cells after 24 h seeding in 25 cm² Falcon flasks (Falcon, Lincoln Park, NJ) were added with the incubation medium containing 3% FCS, as well as with predetermined NiNc concentrations in DPPC liposomes and incubated for 18 or 48 h at 37 °C in a dark humid atmosphere containing 5% CO₂. At the end of the incubation period, the medium was removed and the cell monolayer was carefully washed three times with cold phosphate-buffered saline (PBS). The trypsinised cells were centrifuged, resuspended in 0.5 ml of 2% aqueous sodium dodecyl sulphate (SDS, Prolabo, Fontenay-sous-Bois, France) and magnetically stirred for 1 h at room temperature. Each sample was subdivided into two portions: 0.2 ml was stored for protein determination by the bicinchoninic acid (BCA) assay [26], while 0.3 ml was analysed spectrophotometrically by recording the absorption spectrum in the 500–950 nm range. The naphthalocyanine recovery was expressed as nanomoles of photosensitizer per mg of protein after calculation from a calibration curve. Previous investigations [24] showed that this procedure yielded a quantitative extraction of the naphthalocyanine into the surfactant micelles.

In order to investigate the subcellular distribution of NiNc, the naphthalocyanine-loaded cells were layered on a cover glass and observed by an optical microscope

(Zeiss) in a clear field. The analysis was performed with cell samples that had been incubated with NiNc for 18 or 48 h. The location of NiNc was identified by the appearance of yellowish-brown spots. The spots were attributed to NiNc since (a) no such spots were detectable in cells that had not been incubated with the naphthalocyanine and (b) the colour intensity and number of spots increased with increasing intracellular NiNc concentration.

2.3. Cell photosensitisation studies

The photothermal sensitisation studies with NiNc-incubated and control unsensitised cells were performed by means of a Q-switched Ti:sapphire laser tuned at 850 nm and operated in a pulsed mode (30 ns pulses, 10 Hz) with an energy of 120 mJ/pulse. Typically, the cells were seeded and incubated in 25 cm² flasks as described above. After incubation with NiNc, the flasks were rinsed once with Ca²⁺- and Mg²⁺-free PBS and treated with an aqueous solution (0.6 ml) containing 0.05% trypsin and 0.02% EDTA (Seromed, Berlin). The action of trypsin was stopped by addition of FCS (0.6 ml) and the cell suspension was collected in a 1-cm quartz cuvette and irradiated under gentle magnetic stirring for different time intervals. At the end of irradiation, cell survival was determined by trypan blue exclusion test [27]. The control and photothermally sensitised cells were fixed in 3% glutaraldehyde, post-fixed in 1% osmium tetroxide and dehydrated by graded ethanol solutions. The specimens were gold-coated to improve the resolution and analysed with a scanning electron microscope (Phillips XL30/EDAX DX4i).

2.4. Studies on tumour-bearing mice

Female C57/BL6 mice (20–22 g body weight, supplied by Charles River, Como, Italy) were subcutaneously injected in the upper flank with 10⁶ amelanotic melanoma cells (B78H1) suspended in 20 µl sterile D-MEM. At about 15 days after cell implantation, when the tumour diameter was in the 0.4–0.6 cm range, the mice (at least five mice per group) were injected in the caudal vein with DPPC liposome-incorporated NiNc (1.8 mg/kg body

Table 1
Accumulation and physical state of NiNc in selected cell lines under different incubation conditions

| Cell line | Characteristics | Recovery | | Predominant state | |
|-----------|-----------------------------------|--------------|--------------|-------------------|------------|
| | | A | B | A | B |
| B78H1 | Amelanotic melanoma, murine | 3.06 ± 0.06 | 3.31 ± 0.19 | Monomer | Aggregated |
| C32 | Amelanotic melanoma, human | 10.88 ± 0.97 | 11.74 ± 0.41 | Aggregated | Aggregated |
| HT-1080 | Transformed fibroblasts, murine | 6.95 ± 0.56 | 8.14 ± 0.53 | Monomer | Monomer |
| HaCaT | Transformed keratinocytes, murine | 13.87 ± 0.40 | 6.02 ± 0.50 | Monomer | Monomer |

NiNc = Ni(II)-5,9,14,18,23,27,32,36-octabutoxy-2,3-naphthalocyanine.

Incubation conditions: A = NiNc 7.7 µM, 18 h; B = NiNc 5.1 µM, 48 h. Recoveries are expressed as nmol NiNc/mg of cell protein. The monomeric/aggregated state of the NiNc was probed by absorption spectroscopy of cell-bound naphthalocyanine (see Figs. 3(a) and (b)).

weight). In all cases, the mice were kept in standard cages with free access to tap water and normal dietary chow. At 24 h after injection, the tumour area was irradiated for 140 s by the Ti:sapphire laser (30 ns pulses, 10 Hz, 100 mJ/pulse). An identical irradiation protocol was used for a group of tumour-bearing mice that had not received NiNc. The tumour response was assessed by following the rate of amelanotic melanoma growth as a function of post-irradiation time using a calliper to measure the volume of the lesion at daily intervals. Individual tumour volumes were calculated assuming a hemiellipsoidal structure for the tumour nodule and measuring the two perpendicular axes (a and b) and the height (c). Tumour volume was obtained by the relationship $V = 4/3\pi(a/2 \times b/2 \times c/2)$. The mice were sacrificed when the tumour volume approached 20% of the mouse body weight in line with the rules established by the University of Padova ethical committee for humane treatment of experimental animals. No case had a spontaneous regression of the transplanted tumour.

2.5. Statistical analysis

All data are reported as means \pm standard deviation (s.d.).

3. Results

3.1. Naphthalocyanine uptake by cells

The uptake of NiNc by B78H1 amelanotic melanoma cells as a function of the naphthalocyanine concentration after 18 and 48 h incubation periods was tested. Clearly, the amount of cell-bound NiNc steadily increased up to at least 7.7 μ M, which was the highest test concentration used at both incubation times (Fig. 2).

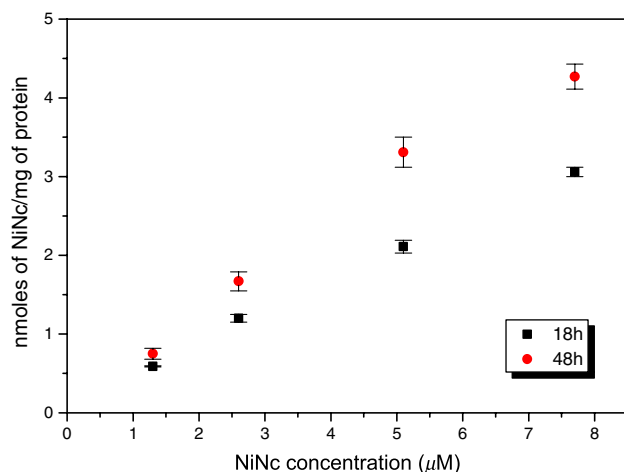


Fig. 2. Effect of NiNc concentration on the accumulation of the naphthalocyanine by B78H1 cells after 18 and 48 h incubation.

This behaviour was observed for several transformed murine (B78H1, HT-1080, HaCaT) or human (C32) cell lines and similar intracellular concentrations were obtained upon incubation of the different cells for 18/48 h with 5.1 or 7.7 μ M NiNc. One notable exception was the results from HaCaT cells, where approximately 50% lower recovery of NiNc was obtained from the 48 h incubated sample (Table 1). In no sample did the naphthalocyanine-loaded cells undergo any appreciable decreases in survival and indicated that NiNc caused no toxic effects on the various cell types in the dark.

In 18 h incubated B78H1 cells, NiNc appeared to be largely monomeric, as shown by the clearly resolved Q-band in the visible absorption spectrum obtained from readings of the naphthalocyanine-loaded cells against a sample of non-incubated cells (Fig. 3(a)). This band underwent a bathochromic shift and a marked broadening after 48 h incubation period (Fig. 3(b)), which suggested a spectral pattern typical of aggregated naphthalocyanines [28]. The flat tetraaza-benzoindole macrocycle is known to favour the formation of stacked or pseudomicellar naphthalocyanine complexes as a result of hydrophobic and π - π interactions, especially in relatively polar microenvironments. The oligomerisation process can be further favoured by the trend of the cell-bound naphthalocyanine molecules to gradually partition to specific subcellular regions. This was clearly demonstrated by optical microscope analysis of NiNc-incubated B78H1 cells, where the pattern of photosensitizer distribution was identified by the presence of typical NiNc dark yellow spots that were absent in control cells (Fig. 4(a₁)). In 18 h incubated B78H1 cells, the spots were seen throughout the cell except the nucleus (Fig. 4(a₂)) and confirmed the observation that naphthalocyanines preferentially partitioned to subcellular membranes [29]. After 48 h incubation, the spots increased in size and were often concentrated in limited cellular areas for most detectable cells, a process that should facilitate the stacking of the photosensitizer molecules (Fig. 4(a₃)). The extent and kinetics of NiNc distribution differed for different cell types. For amelanotic melanoma C32 cells (Fig. 4(b)), a significant degree of NiNc compartmentalisation was already evident after 18 h incubation (Fig. 4(b₂)) and this pattern underwent minor changes upon prolonged incubation to 48 h (Fig. 4(b₃)). This finding was in good agreement with the predominantly aggregated shape of the NiNc absorption spectrum at 48 h incubation time for C32 cells (Fig. 3(c)). Peculiarly, in HaCaT keratinocytes (Fig. 4(c)) and HT1080 fibroblasts (data not shown), the cell-bound NiNc gave a monomeric-type absorption spectrum (Fig. 3(d)) and also appeared to remain finely dispersed at least up to 48 h incubation (Figs. 4(c₂) and (c₃)). The prevalent monomeric or aggregated feature of the visible absorption spectrum of cell-bound NiNc is summarised in Table 1.

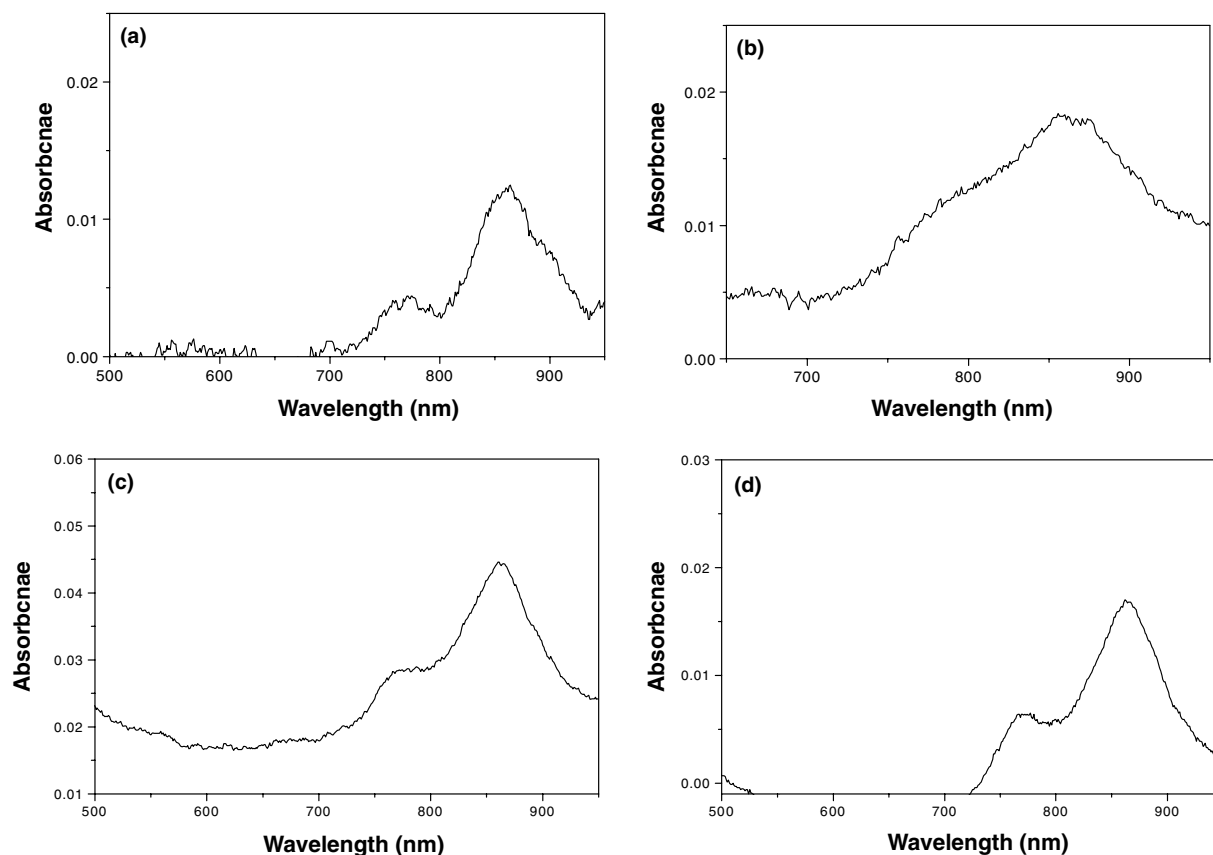


Fig. 3. Absorption spectrum in the visible range of cells incubated with $7.7 \mu\text{M}$ naphthalocyanine. NiNc bound to B78H1 cells after (a) 18 h, (b) 48 h and (c) C32 cells (d) HT1080 cells after 48 h.

3.2. Cell photosensitisation studies

On the basis of the binding/distribution studies, the cells were exposed to irradiation after incubation with $7.7 \mu\text{M}$ NiNc for 18 h and $5.1 \mu\text{M}$ NiNc for 48 h i.e., under experimental conditions yielding fairly similar intracellular molar concentrations of the photosensitizer (Table 1). Preliminary studies showed that irradiation of NiNc-loaded B78H1 amelanotic melanoma cells for 30 min with 850 nm from a c.w. operated Ti:sapphire laser caused no appreciable decrease in cell survival in spite of the efficient accumulation of the naphthalocyanine. Similarly, as a control, 20 min irradiation of the various cell lines with the Ti:sapphire operated in the pulsed regime (see Section 2) and in the absence of NiNc had no effect on cell survival. It seemed that no photodynamic process or thermal effects were induced by irradiation with pulsed high intensity 850 nm light under these experimental conditions. On the other hand, exposure of the cells, which had been incubated with NiNc, to pulsed 850 nm light invariably induced cytotoxic effects (Figs. 5(a) and (b)). The degree of cell mortality was particularly extensive for those samples (18 and 48 h C32 human amelanotic melanoma cells, 48 h B78H1 murine amelanotic melanoma cells) where the

naphthalocyanine was aggregated and/or compartmentalised (Figs. 3 and 4). The photoprocess was very efficient since less than 10% residual survival was measured after 1 min exposure to light. The weight of these factors appears to be far greater than that of the intracellular naphthalocyanine concentration, since B78H1 cells ($3.31 \text{ nmol NiNc/mg protein}$) were significantly more photosensitive than HaCaT cells (13.87 or 6.02 nmol) or HT-1080 cells (6.95 or 8.14 nmol).

Such a high level of cell photosensitivity could reflect the mechanisms controlling photothermal sensitization. Scanning electron microscopy analysis showed that control and unsensitized but irradiated C32 cells (Figs. 6(a) and (b)) exhibited a regular spherical shape. However, after 1 min of irradiation, in 18 h NiNc incubated C32 cells the outward separation of a consistent cellular mass (Fig. 6(c)) followed by formation of a deep hole (Fig. 6(d)) that can reach the cell nucleus was seen. A similar pattern was observed for 48 h incubated cells (Figs. 6(e) and (f)). It is tempting to propose that the images represent the photothermally induced ejection of cytoplasmic material subsequent to the photogeneration of shock waves. When the 1 min irradiated cells were observed by optical microscopy, the expelled material from C32 (Fig. 6(g)) and B78H1 (Fig. 6(h)) cells appeared to be

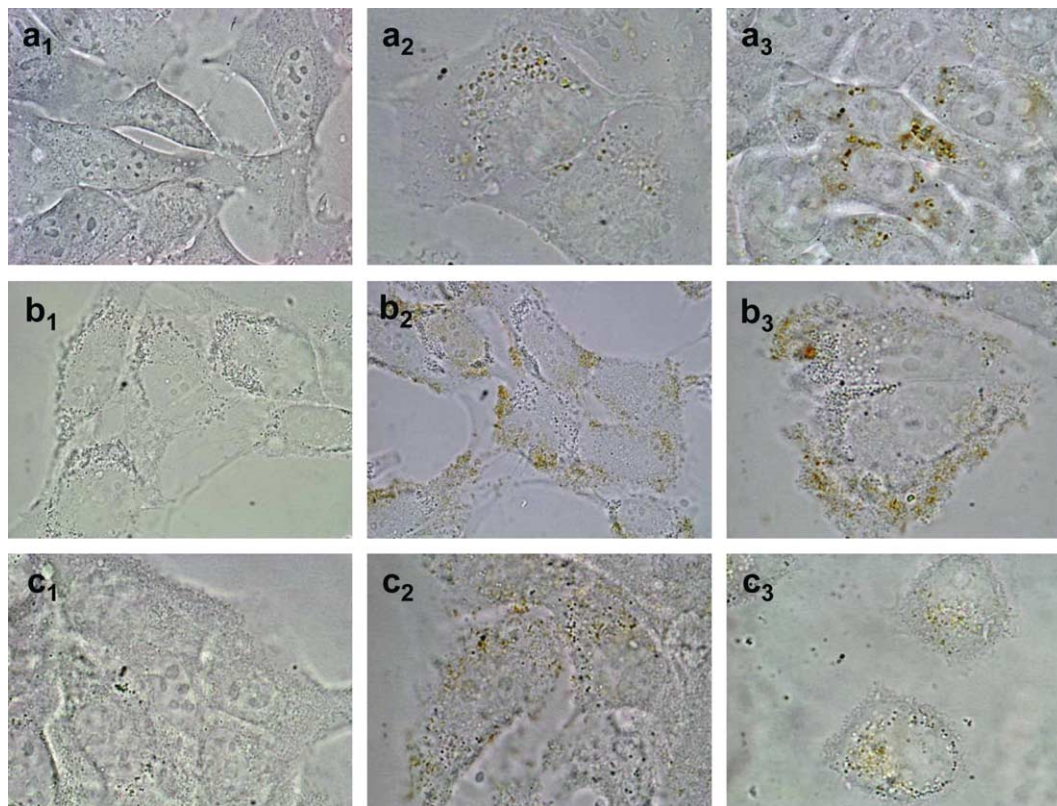


Fig. 4. Subcellular distribution of 7.7 μM NiNc was determined by optical microscope observations in clear field. Panels: (a₁) untreated controls, (a₂) 18 h incubated and (a₃) 48 h incubated B78H1 cells; (b₁) untreated controls, (b₂) 18 h incubated and (b₃) 48 h incubated C32 cells; (c₁) untreated controls, (c₂) 18 h incubated and (c₃) 48 h incubated HaCaT cells.

densely loaded with NiNc. It would appear then that the cytotoxic effects are maximal for cell regions with higher photosensitizer concentrations. Similar alterations of cell morphology were also noted for 48 h incubated and irradiated B78H1, HT-1080 and HaCaT cells (Figs. 6(i)–(n)).

NiNc appeared to be very photostable to pulsed laser irradiation, since the naphthalocyanine could be quantitatively recovered from B78H1 and C32 cells after 20 min irradiation.

3.3. *In vivo* phototherapeutic studies

Photothermal sensitisation of tumours is also effective *in vivo*. Mice bearing a subcutaneous amelanotic melanoma, which were irradiated by the pulsed Ti:sapphire laser 24 h after intravenous (i.v.) injection of 1.8 mg/kg NiNc (the post-injection time interval corresponded to a large accumulation in skin tumours for various naphthalocyanines [30]), displayed an apparently complete disappearance of the lesions with initial eschar formation indicative of massive hemorrhagic necrosis (Fig. 7). Measurement of the intratumoural temperature by a thermocamera during pulsed Ti:sapphire irradiation indicated that the temperature of the NiNc-loaded neoplastic lesion rose to approximately

105 °C within 80 s, remained essentially stable until the end of irradiation (140 s) and returned to basal temperature (approximately 32 °C) within 1 min after tumour exposure to light was interrupted. The temperature spike obtained was markedly hotter than that measured for the same tumour (45–48 °C) when the irradiations were performed by the Ti:sapphire laser under identical experimental conditions in the absence of NiNc.

Complete healing of the NiNc-photosensitised neoplastic lesion occurred in approximately seven days, suggesting that an extensive photothermally induced damage of the tumour tissue was not accompanied by irreversible damage of the peritumoural districts. Both the tumour-adjacent normal skin and the tissue layers underlying the neoplastic mass were spared, even though the average depth of the melanoma (0.4 cm) was smaller than the penetration depth of 850 nm light (approximately 1 cm in lightly pigmented tumours, see Ref. [31]). It is unlikely that important contributions to tumour response was provided by hyperthermal effects, since irradiation of NiNc-unsensitised mice caused only a minor delay of tumour growth. The photothermal process acted with an unusually high efficiency, since all the NiNc-injected phototreated mice remained tumour-free for about 20 days after irradiation times as short as 140 s. The regrowth of tumours can probably be

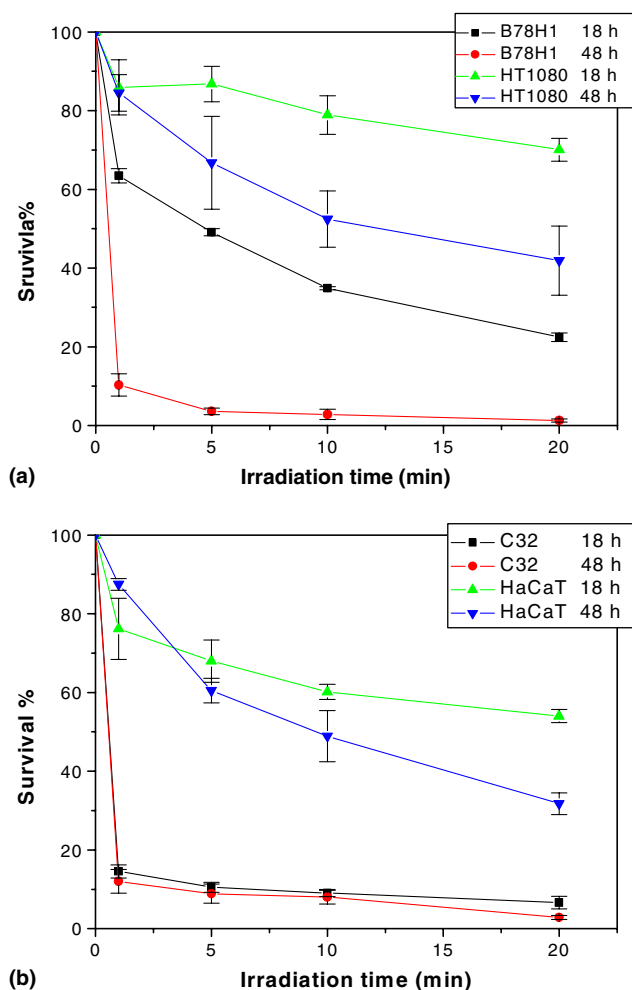


Fig. 5. Photothermal sensitisation of tumour cells *in vitro* by NiNc. Photosensitised inactivation of (a) murine (B78H1, HT-1080) and (b) human (C32, HaCaT) cells upon irradiation (850 nm, 120 mJ, 30 ns pulses) for different periods of time after incubation for 18 h with 7.7 μ M NiNc and 48 h with 5.1 μ M NiNc.

ascribed to the proliferation of small numbers of undamaged or sublethally damaged malignant cells. Normally, the implantation of a melanoma requires ca. 10^6 cells leading to visible detection of the tumour after 1 week.

4. Discussion

The present findings clearly underline that photothermal sensitisation is a very efficient process at both a cellular and animal level and can be usefully applied for the treatment of at least cutaneous tumours. An extensive and irreversible damage to neoplastic cells was achieved *in vitro* and *in vivo* after irradiation times as short as a few minutes with minimal and recoverable damage to the normal tissue surrounding the malignant lesion. The technique was highly selective in space and time and generated extensive and irreversible cell damage

especially when the photosensitizer underwent significant compartmentalisation, which in turn promoted the formation of aggregated photosensitizer clusters. This type of process is especially facilitated in naphthalocyanines that are significantly hydrophobic and are known to localize to inner membranous districts [29,30]. These observations are also in agreement with theoretical predictions, namely the sudden temperature rise in the photosensitizer microenvironment leading to violent water evaporation and the consequent generation of a shock wave. The overall effect is obviously potentiated by the simultaneous development of more than one shock wave in the same subcellular space, as is likely to occur when aggregated derivatives of the photosensitizer are present. Examination of the irradiated cells even after short periods of exposure to light shows the NiNc-promoted release of a consistent mass of cytoplasmic material and related formation of large endocellular cavities (Fig. 6). The photothermal processes promoted under our experimental conditions appear to be markedly different from those typical of a traditional thermal interaction, as shown also by the lack of correlation between the amount of cell-bound naphthalocyanine and overall cell photosensitivity. The temperature rise induced by irradiation with high intensity light in the absence of naphthalocyanine, even though leading to values that are 15–20 °C higher than the basal temperature of the mouse, did not seem to cause a persistent or significant damage, possibly due to the short light exposure time.

To our knowledge, the images obtained with optical and scanning electron microscope are the first experimental demonstration of the mechanisms involved in photothermal sensitisation at a cellular level. The nature of the photodamage precludes the possibility of repair processes or selection of resistant cell clones. Photothermal sensitisation works through a different mode of action on cells compared to photodynamic or radiosensitised processes, where the chemical modification of specific targets is usually ultimately responsible for cell death, which may take place by a variety of apoptotic or random necrotic pathways [32]. The introduction of photothermal drugs would broaden the field of phototherapeutic applications. Photodynamic and radiosensitised therapy require the generation of reactive chemical intermediates and are only efficient in the presence of oxygen [33]. Importantly, photothermal therapy is independent of oxygen concentration in the irradiated system [19] and employs molecular vibrations that are much lower in energy than electronic levels and so even low-lying electronic states can initiate photothermal processes. In principle, polycyclic compounds absorbing far-red or near-infrared light could be used as photothermal sensitizers, whereas the choice of photodynamic sensitizers is limited by the requirement for them to possess sufficiently high-energy triplet states in order

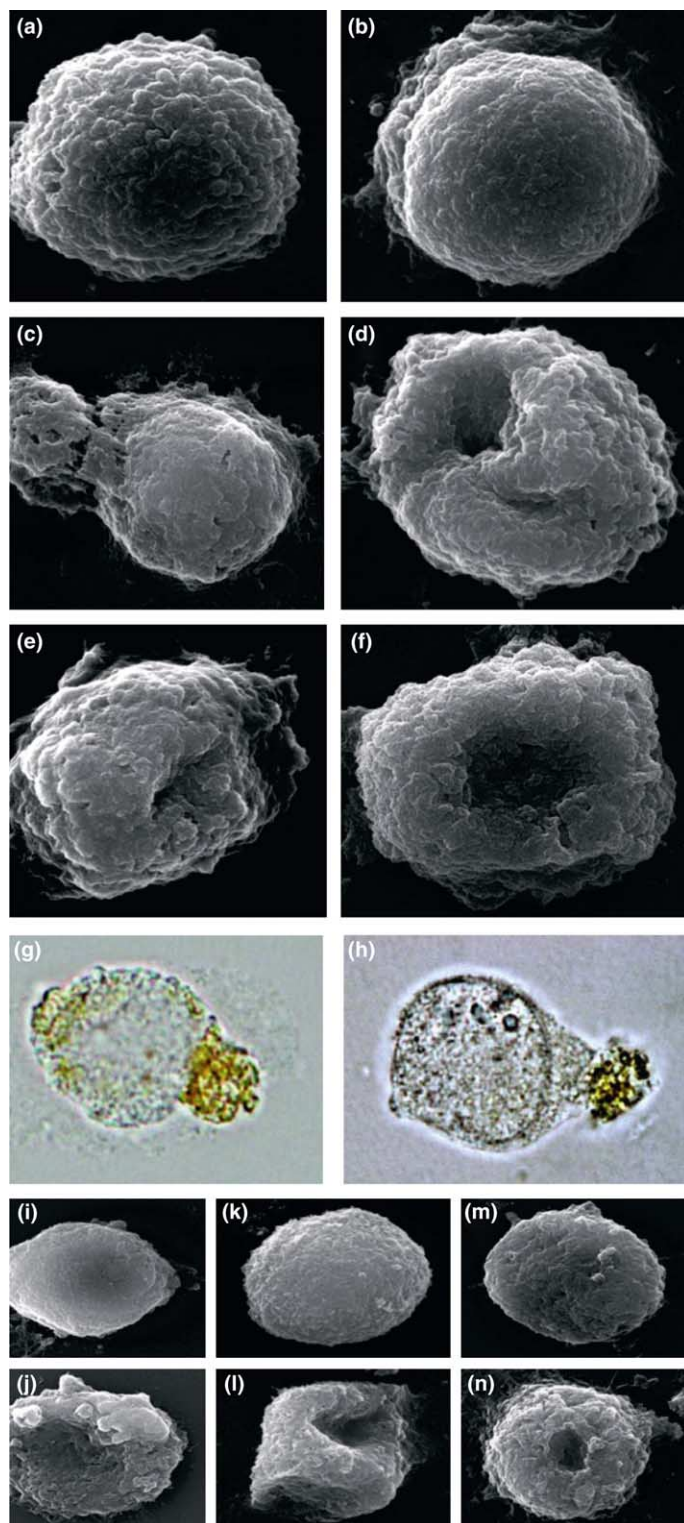


Fig. 6. Morphological alterations in photothermally sensitised tumour cells as studied by scanning electron microscopy (SEM) and optical microscopy (OM). First panel: SEM images of C32 cells (a) untreated controls; (b) irradiated controls in the absence of NiNc; 18 h incubated with 7.7 μ M NiNc and (c) 1 min or (d) 20 min irradiated cells; 48 h incubated with 5.1 μ M NiNc and (e) 1 min or (f) 20 min irradiated cells. Second panel: OM images in clear field of (g) C32 and (h) B78H1 cells irradiated for 1 min after 18 h incubation with 7.7 μ M NiNc. Third panel: SEM images of (i) control and (j) 20 min irradiated B78H1 cells, (k) control and (l) 20 min irradiated HT1080 cells and (m) control and (n) 20 min irradiated HaCaT cells. In all cases, the irradiated cells had been incubated for 48 h with 5.1 μ M NiNc.

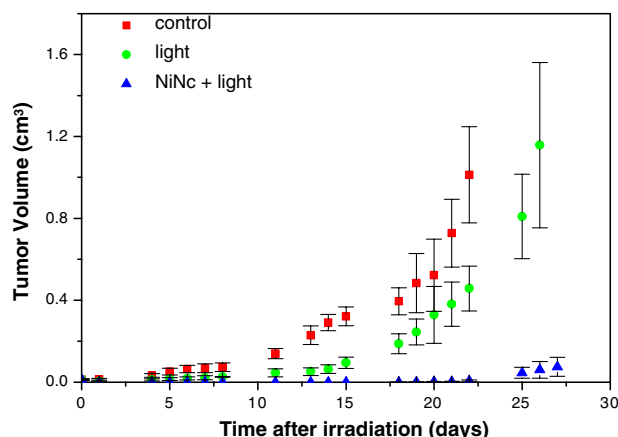


Fig. 7. Rate of tumour growth in C57BL/6 mice bearing a subcutaneously transplanted amelanotic melanoma, that were irradiated (850 nm, 100 mJ, 30 ns pulses) for 140 s in the absence and at 24 h after intravenous injection of NiNc (1.8 mg/kg); the growth rate is compared with that observed for control untreated mice.

to generate the cytotoxic singlet oxygen species via electronic energy transfer [33]. Lastly, the inertness of photothermal sensitizers to cw light (including sunlight) irradiation alleviates the problem of prolonged photosensitivity, which has been an undesired side effect of photodynamic therapy [1,4].

So far, we were unable to determine the pharmacokinetic behaviour of photothermal sensitizers. The lack of detectable fluorescence emission by these compounds makes it very difficult to measure their concentrations in tumours and healthy tissues by the traditional spectrofluorimetric analysis either directly *in vivo* [34] or after chemical extraction from tissue homogenates [30]. However, it appears reasonable to expect that the time-dependence of *in vivo* distribution of NiNc or other photothermally acting metallo-naphthalocyanines is very similar to other typical naphthalo- and phthalocyanines that have photodynamic properties (e.g., the Si(IV), Zn(II) or Ge(IV) derivatives), all of which exhibit essentially identical kinetics of accumulation and clearance from a variety of experimental tumours [35]. In our case, the irradiation of subcutaneously transplanted amelanotic melanoma at 24 h after i.v injection of NiNc, yielded a satisfactory tumour response as observed for several PDT treatments. Such a close similarity in the pharmacokinetic properties, coupled with the large differences in the photosensitisation mechanism, opens the possibility to develop a combined therapeutic protocol, involving the sequential treatment of a tumour by PDT and PTT. The simultaneous administration of a photothermal and photodynamic sensitizer differing only in the nature of the metal ion coordinated with the naphthalocyanine (or similar) macrocycle could be of therapeutic value. These approaches could complement other previously proposed techniques, such as indocyanine green-assisted laser therapy that share the use of near-infrared radiation as the photoactivating light [17].

Conflict of interest statement

None declared.

Acknowledgement

Partial support for this work was obtained from NIH Grant CA 91027.

References

1. Moor AC, Ortel B, Hasan T. Mechanisms of photodynamic therapy. In Patrice T, ed. *Photodynamic Therapy*. Cambridge, The Royal Society of Chemistry, 2003. pp. 19–57.
2. Peng Q, Warloe T, Berg K, et al. 5-Amino-levulinic acid-based photodynamic therapy: clinical research and future challenges. *Cancer* 1997, **79**, 2282–2308.
3. Dougherty TJ, Gomer CJ, Jori G, et al. Photodynamic therapy. *J Natl Cancer Inst* 1998, **90**, 889–905.
4. Calzavara PG, Szeimies RM, Ortel B. *Photodynamic Therapy and Fluorescence Diagnosis in Dermatology*. Cambridge, Royal Society of Chemistry, 2001.
5. Jori G, Brown SB. Photosensitized inactivation of microorganisms. *Photochem Photobiol Sci* 2004, **3**, 403–405.
6. Valassis G, Pragst I, Adolfs C, et al. Local photodynamic therapy reduces tissue hyperplasia after stenting in an experimental restenosis model. *Basic Res Cardiol* 2002, **97**, 132–136.
7. Boyle RW, Dolphin D. Structure and biodistribution relationships of photodynamic sensitizers. *Photochem Photobiol* 1996, **64**, 469–485.
8. Ma LW, Moan J, Steen HB, et al. Anti-tumour activity of photodynamic therapy in combination with mitomycin c in nude mice with human colon adenocarcinoma. *Br J Cancer* 1995, **71**, 950–956.
9. Schaffer M, Ertl-Wagner B, Kulka U, et al. Porphyrins as radiosensitising agents for solid neoplasms. *Curr Pharm Design* 2003, **9**, 2024–2035.
10. Soncin M, Busetti A, Fusi F, et al. Irradiation of amelanotic melanoma cells with 532 nm high peak power pulsed laser radiation in the presence of the photothermal sensitizer Cu (II)-haematoporphyrin: a new approach to cell photoinactivation. *Photochem Photobiol* 1999, **69**, 708–712.
11. Okazaki T, Hirota N, Nagata T, et al. High temporally and spatially resolved thermal energy detection after non-radiative transition in solution using a molecular heater-molecular thermometer integrated system. *J Am Chem Soc* 1999, **121**, 5079–5080.
12. Drain CM, Rockwell S, Cheng G, et al. Picosecond to microsecond photodynamics of a non-planar nickel-porphyrin: solvent dielectric and temperature effects. *J Am Chem Soc* 1998, **120**, 3781–3791.
13. Goldberg TJ. Laser treatment of pigmented lesions. *Dermatol Clin* 1997, **15**, 397–407.
14. Dierickx CC, Casparian JM, Venugopalan V, et al. Thermal relaxation of port-wine vessels probed *in vivo*: the need for 1–10 millisecond laser pulse treatment. *J Invest Dermatol* 1995, **105**, 709–714.
15. Jori G, Spikes JD. Photothermal sensitizers: possible use in tumour therapy. *J Photochem Photobiol B: Biol* 1990, **6**, 93–101.
16. Chen WR, Adams RL, Carubelli R, et al. Laser-photosensitizer assisted immunotherapy. A novel modality in cancer treatment. *Cancer Lett* 1997, **115**, 25–30.

17. Chen WR, Jeong SW, Lucroy MD, et al. Induced anti-tumour immunity against DMBA-4 metastatic mammary tumours in rats using a novel approach. *Int J Cancer* 2003, **107**, 1053–1057.
18. Moan J, Sommer S. Oxygen dependence of the photosensitising effect of haematoporphyrin derivative in NHIK 3025 cells. *Cancer Res* 1985, **45**, 1608–1610.
19. Camerin M, Rodgers MAJ, Kenney ME, et al. Photothermal sensitisation: evidence for the lack of oxygen effect on the photosensitizing activity. *Photochem Photobiol Sci* 2005, **4**, 251–253.
20. Buseti A, Soncin M, Jori G, et al. Treatment of malignant melanoma by high-peak-power 1064 nm irradiation followed by photodynamic therapy. *Photochem Photobiol* 1998, **68**, 377–381.
21. Star WM. Light dosimetry *in vivo*. *Phys Med Biol* 1997, **42**, 763–787.
22. Jori G, Schindl L, Schindl A, et al. Novel approaches towards a detailed control of the mechanism and efficiency of photosensitized processes *in vivo*. *J Photochem Photobiol A: Chem* 1996, **102**, 101–107.
23. Aoudia M, Cheng G, Kennedy VO, et al. Synthesis of a series of octabutoxy-benzophthalocyanines and photophysical properties of two members of the series. *J Am Chem Soc* 1997, **119**, 6029–6039.
24. Buseti A, Soncin M, Reddi E, et al. Photothermal sensitisation of amelanotic melanoma cells by Ni (II)-octabutoxy-naphthalocyanine. *J Photochem Photobiol B: Biol* 1999, **53**, 103–109.
25. Kremer JMH, Esker MWJ, Pathmanoharan C, et al. Vesicles of variable diameter prepared by a modified injection method. *Biochemistry* 1997, **16**, 3932–3935.
26. Smith PH, Krohn RI, Hermanson GT, et al. Measurement of protein using bicinchoninic acid. *Anal Biochem* 1985, **150**, 76–85.
27. Rockwell S. *In vivo* and *in vitro* tumour cell lines: characteristics and models for human cancer. *Br J Cancer* 1980, **41**, 118–126.
28. Reddi E, Jori G. Steady-state and time-resolved spectroscopic studies of photodynamic sensitizers: porphyrins and phthalocyanines. *Rev Chem Interim* 1988, **10**, 241–268.
29. Jori G. Tumour photosensitizers: approaches to enhance the selectivity and efficiency of photodynamic therapy. *J Photochem Photobiol B: Biol* 1996, **36**, 87–93.
30. Soncin M, Buseti A, Biolo R, et al. Photoinactivation of amelanotic and melanotic melanoma cells sensitized by axially substituted Si-naphthalocyanines. *J Photochem Photobiol B: Biol* 1998, **42**, 202–210.
31. Wilson BC. Technologies and biophysical techniques for PDT. In Patrice T, ed. *Photodynamic Therapy*. Cambridge, Royal Society of Chemistry, 2003. pp. 127–157.
32. Oleinick NL, Morris RL, Belichenko I. The role of apoptosis in response to photodynamic therapy: what, where, why, and how. *Photochem Photobiol Sci* 2002, **1**, 1–21.
33. Oleinick NL, Evans HH. The photobiology of photodynamic therapy: cellular targets and mechanisms. *Radiat Res* 1998, **150**, 146–156.
34. Sutedja G. Fluorescence bronchoscopy for early detection of lung cancer. In Patrice T, ed. *Photodynamic Therapy*. Cambridge, Royal Society of Chemistry, 2003. pp. 159–175.
35. Biolo R, Jori G, Soncin M, et al. Effect of photosensitizer delivery system and irradiation parameters on the efficiency of photodynamic therapy of B16 pigmented melanoma in mice. *Photochem Photobiol* 1996, **63**, 224–228.